

Journal of
Applied Remote Sensing

**Terra and Aqua moderate-resolution
imaging spectroradiometer collection 6
level 1B algorithm**

Gary Toller
Xiaoxiong Xiong
Junqiang Sun
Brian N. Wenny
Xu Geng
James Kuyper
Amit Angal
Hongda Chen
Sriharsha Madhavan
Aisheng Wu



Terra and Aqua moderate-resolution imaging spectroradiometer collection 6 level 1B algorithm

Gary Toller,^a Xiaoxiong Xiong,^b Junqiang Sun,^a Brian N. Wenny,^a
Xu Geng,^a James Kuyper,^a Amit Angal,^c Hongda Chen,^a
Sriharsha Madhavan,^c and Aisheng Wu^a

^aSigma Space Corporation, 4801 Forbes Boulevard, Lanham, Maryland 20706
gtoller@sigmaspace.com

^bSciences and Exploration Directorate, NASA/Goddard Space Flight Center, Greenbelt,
Maryland 20771

^cScience Systems and Applications Inc., 10210 Greenbelt Road, Lanham, Maryland 20706

Abstract. The moderate-resolution imaging spectroradiometer (MODIS) was launched on the Terra spacecraft on Dec.18, 1999 and on Aqua on May 4, 2002. The data acquired by these instruments have contributed to the long-term climate data record for more than a decade and represent a key component of NASA's Earth observing system. Each MODIS instrument observes nearly the whole Earth each day, enabling the scientific characterization of the land, ocean, and atmosphere. The MODIS Level 1B (L1B) algorithms input uncalibrated geo-located observations and convert instrument response into calibrated reflectance and radiance, which are used to generate science data products. The instrument characterization needed to run the L1B code is currently implemented using time-dependent lookup tables. The MODIS characterization support team, working closely with the MODIS Science Team, has improved the product quality with each data reprocessing. We provide an overview of the new L1B algorithm release, designated collection 6. Recent improvements made as a consequence of on-orbit calibration, on-orbit analyses, and operational considerations are described. Instrument performance and the expected impact of L1B changes on the collection 6 L1B products are discussed. © 2013 Society of Photo-Optical Instrumentation Engineers (SPIE) [DOI: [10.1117/1.JRS.7.073557](https://doi.org/10.1117/1.JRS.7.073557)]

Keywords: moderate-resolution imaging spectroradiometer; Terra; Aqua; remote sensing; data processing; satellite.

Paper 12446 received Nov. 28, 2012; revised manuscript received Apr. 10, 2013; accepted for publication Apr. 19, 2013; published online May 22, 2013.

1 Introduction

The moderate-resolution imaging spectroradiometer (MODIS) is the key instrument on NASA's Earth-orbiting Terra and Aqua satellites. MODIS uses 490 detectors distributed among 36 spectral bands and on-board calibrators in support of land, ocean, and atmospheric studies. Both MODIS instruments are still operating nominally and provide valuable, nearly daily global coverage data to the science community. Descriptions of the MODIS bands, system design, and mission observational characteristics are available.^{1,2}

The MODIS adaptive processing system (MODAPS) geo-locates and reformats Level 0 data into hierarchical data format (HDF-4) Level 1A files. The Level 1B (L1B) software converts this raw instrument data into top of the atmosphere (TOA) calibrated radiance for all bands and into reflectance for the 20 reflected solar bands (RSBs). Similar but distinct Terra and Aqua versions of the L1B software and lookup tables (LUTs) address the unique operational configurations and characteristics of the two instruments.

The MODIS characterization support team (MCST) developed the L1B software and is responsible for its maintenance and improvement. Significant code and LUT upgrades are based on MODIS data analysis, continuous monitoring of the aging instruments, on-orbit

calibrations, improved instrument characterization, and input from the science team. This leads to a new L1B collection that includes data reprocessing as well as forward processing in an effort to provide the best data products available at the time. This paper describes the improvements made to produce the L1B collection 6 (C6) software. This paper extends the description of previous L1B updates³ and L1B algorithm descriptions⁴⁻⁷ to the current C6 version of L1B.

Section 2 presents the MODIS on-orbit calibration methodology, followed by the instrument performance in Sec. 3. Section 4 provides a description of the L1B data products. Section 5 discusses the recent improvements made to Terra and Aqua L1B and the impact on the data products. Section 6 highlights the lessons learned over the course of L1B development. Conclusions are provided in Sec. 7.

2 On-Orbit Calibration

Calibration is performed on a pixel-by-pixel basis for each detector. The detectors are located on one of four focal plane assemblies (FPAs) covering the visible (VIS), near-infrared (NIR), short- and mid-wavelength infrared (SWIR/MWIR), and long-wavelength infrared (LWIR) spectral regions. Bands 1 to 19 and band 26 are the reflective solar bands (RSBs). Bands 20 to 25 and 27 to 36 are the thermal emissive bands (TEBs). Measured characteristics for MODIS Terra and Aqua bands have previously been provided.^{8,9} Each pixel is calibrated and indexed according to band, detector, subsample (for the subkilometer high resolution bands 1-7), and mirror side (MS). Uncertainties in the calibrated radiance and reflectance are provided for each pixel.

Spatial, spectral, and radiometric calibration for each Terra and Aqua MODIS detector are provided by its on-board calibrators. The calibrators consist of a solar diffuser (SD) combined with a SD stability monitor (SDSM), a blackbody (BB), and a spectral radiometric calibration assembly (SRCA). Specific aspects of calibration, such as characterization of the instrument response versus scan angle (RVS), electronic crosstalk, and optical leak are studied using these calibrators. Once in orbit, observations of the Moon and Earth-view (EV) vicarious calibration sites also support instrument calibration and characterization.

Information about MODIS instrument characteristics and performance, a description of the current L1B versions, features of the science data products, and key MCST documents, presentations, and references are available online.¹⁰ The calibration design requirements at typical radiance levels are 2% for RSB reflectance, 5% for RSB radiance, and 1% for TEB radiances (except 0.5% for bands 31 and 32, 0.75% for band 20, and 10% for the fire detection band 21). Calibration accuracy throughout both missions meets these requirements, except for bands with known anomalies.

With every scan, MODIS observes the Earth, deep space (a zero signal), the on-board BB, the SRCA, and the SD. The BB provides the scan-by-scan TEB calibration.^{11,12} The SRCA allows for detailed on-orbit characterization of the detectors' radiometric, spatial, and spectral properties over time.^{13,14} The SD and SDSM, supplemented by lunar observations, form the basis for RSB calibration.¹⁵⁻¹⁷

The primary L1B TEB product is the TOA radiance, L_{EV} . The equation¹⁸ used to solve for L_{EV} is

$$RVS_{EV} \cdot L_{EV} + (RVS_{SV} - RVS_{EV}) \cdot L_{SM} = a_0 + b_1 \cdot dn_{EV} + a_2 \cdot dn_{EV}^2, \quad (1)$$

where RVS is the response versus scan angle of the mirror normalized to the angle of incidence (AOI) of the BB; the subscripts EV and SV represent the earthview and spaceview, respectively; L_{SM} is the emission of the scan mirror; a_0 is the offset calibration coefficient; b_1 is the linear gain coefficient computed each scan from observations of the BB; a_2 is the quadratic term coefficient; and dn_{EV} is the EV minus the scan-averaged SV digital numbers. On-orbit calibration of the 160 TEB detectors is performed for each scan using a quadratic fit to the known radiance emitted by the on-board BB. Quarterly BB warmup, cooldown (WUCD) cycles enable the compilation of TEB detector responses to temperatures ranging from 270 K to 315 K. This dataset is applied in LUT updates and allows for the determination of a_0 and a_2 . These coefficients subsequently determine L_{EV} .

The principal L1B RSB product is the EV TOA reflectance factor, $\rho_{EV} \cdot \cos(\theta_{EV})$, which is calculated using

$$\rho_{EV} \cdot \cos(\theta_{EV}) = dn'_{EV} \cdot d_{ES}^2 \cdot m_1 / RVS, \quad (2)$$

where ρ_{EV} is the Earth scene bi-directional reflectance factor, θ_{EV} is the solar zenith angle of the EV pixel, dn'_{EV} is the sensor's response corrected for the effects of instrument background and temperature, d_{ES} is the Earth-Sun distance in AU at the time of the EV observation, m_1 is the calibration coefficient supplied by a time-dependent LUT derived and updated in orbit from the SD/SDSM calibration, and RVS is normalized to the AOI of the SD. The instrument gain at the SD AOI is proportional to $1/m_1$. SD/SDSM and lunar calibrations track the on-orbit gain changes at the AOIs of the SD and the SV. The RSB RVS on-orbit variations are derived from the SD/SDSM and lunar calibrations, plus the response trending obtained from EV observations for select RSB.

3 On-Orbit Performance

Increased understanding of instrument behavior and analysis of changes in instrument response over time have led to improvements in the L1B code and the LUTs. Instrument performance is assessed by trending key quantities, such as temperature and gain information, through the examination of EV data and by feedback received from the science team. These quality assurance (QA) activities are the basis for the Detector Quality Flag LUTs, which indicate that, after more than 12 and 10 years of operation, respectively, 488 of the 490 Terra MODIS detectors and 476 of the 490 Aqua MODIS detectors still provide usable data. The on-board calibrators continue to operate nominally. Both short- and long-term stability remain excellent throughout both missions. Because of lessons learned from the Terra MODIS program, the Aqua MODIS performance is superior in terms of stability and calibration accuracy.

Table 1 provides performance data for Terra and Aqua MODIS during four time periods: prelaunch (PL), annually averaged for the first year of operation, and the years 2008 and 2011. The signal-to-noise (SNR) values given for these periods are ratios compared to the SNR specification (spec). Therefore, values above 1 are desirable. The small deficiency in Terra band 7 was identified before launch. The decrease in SNR over time for several bands is mostly due to the decrease of detector gain, as illustrated in Figs. 1 and 2, and should not be misconstrued as indicating noisy detectors. The noise equivalent temperature variance (NEdT) values in Table 1 are ratios of the measured NEdT to the NEdT spec. NEdT values below 1 indicate satisfactory performance. The somewhat high noise level in Terra band 36 was a known issue before launch. Table entries are based on all operational detectors, excluding noisy detectors. The number of detectors characterized as noisy is time dependent but has never exceeded seven of the 490 Aqua detectors or 29 of the 490 Terra detectors.¹⁰ The overall performance remains satisfactory throughout both missions.

An example of gain trending since the first data collection is provided in Fig. 1. The trend for Terra MODIS RSB VIS band responses as a function of time is depicted for mirror side 1 (MS1). The dashed vertical lines in the figure indicate some of the key instrument events. The color-coded band data have been averaged over all good detectors in the band. The abscissa is the number of days since launch. Gains are normalized to 1.0 at the first collection of data. The gain deterioration for Terra grows after the SD door is fixed to the open position 1,292 days after launch (July 2, 2003). The normalized gain as a function of time for MS2 has very similar characteristics to Fig. 1. Gain variations during the mission are corrected by submitting time-dependent LUT updates.

The Aqua RSB VIS band FPA gain trend for MS1 (and indistinguishable from MS2) is provided in Fig. 2. It is apparent that the long-term changes in Aqua are much smaller than those in Terra.

For both missions, the changes in the properties of the scan mirror are larger for the shorter wavelengths. Analysis also reveals that larger MS differences are observed in the short-wavelength bands at larger AOI. The L1B calibration process corrects for the gain changes for each band and detector as a function of MS, time, and AOI.

Table 1 SNR and NEdT specifications and performance for each band (B).

RSB B	SNR spec	Terra				Aqua			
		PL	2000	2008	2011	PL	2002	2008	2011
1	128	1.42	1.50	1.59	1.63	1.34	1.55	1.57	1.65
2	201	2.41	2.45	2.60	2.64	2.27	2.54	2.69	2.75
3	243	1.42	1.36	1.14	0.91	1.31	1.32	1.23	1.18
4	228	1.48	1.48	1.31	1.22	1.91	1.42	1.41	1.41
5	74	1.32	1.31	1.13	1.14	1.12	2.05	2.01	1.96
6	275	1.42	0.92	1.23	1.19	1.54	1.65	1.74	1.62
7	110	0.90	0.94	0.91	0.90	1.60	1.40	1.41	1.40
8	880	1.26	1.12	0.71	0.77	1.21	1.27	1.01	0.85
9	838	1.85	1.53	1.20	1.05	1.75	1.84	1.63	1.51
10	802	1.96	1.52	1.39	1.26	1.52	1.94	1.83	1.79
11	754	2.17	1.61	1.57	1.49	1.41	2.29	2.26	2.25
12	750	2.00	1.38	1.30	1.19	1.41	2.03	1.98	1.97
13	910	1.29	1.15	1.19	1.19	1.37	1.58	1.63	1.65
14	1087	1.21	1.04	0.98	0.95	1.15	1.45	1.45	1.46
15	586	2.14	1.76	1.73	1.72	1.94	2.68	2.74	2.75
16	516	2.16	1.75	1.74	1.75	1.95	2.78	2.84	2.84
17	167	2.17	2.20	2.11	2.07	1.87	2.20	2.25	2.24
18	57	1.58	1.68	1.70	1.75	2.08	1.60	1.61	1.62
19	250	2.06	2.11	2.05	2.02	1.60	2.03	2.05	2.06
26	150	1.57	1.66	1.69	1.66	2.32	1.85	1.90	1.90
TEB B	NEdT spec	PL	2000	2008	2011	PL	2002	2008	2011
20	0.05	.507	.548	.507	.508	.384	.476	.477	.467
21	0.20	.844	.812	.777	.788	1.18	1.03	1.07	.950
22	0.07	.385	.425	.372	.374	.241	.286	.281	.282
23	0.07	.341	.342	.341	.341	.249	.293	.292	.291
24	0.25	.508	.635	.521	.522	.501	.437	.432	.428
25	0.25	.238	.225	.203	.203	.144	.160	.155	.155
27	0.25	.417	.340	.429	.407	.355	.392	.365	.400
28	0.25	.173	.222	.301	.259	.197	.189	.183	.192
29	0.05	.439	.475	.553	.535	.331	.402	.431	.429
30	0.25	.364	.392	.471	.535	.341	.331	.333	.386
31	0.05	.579	.517	.505	.505	.468	.335	.335	.337
32	0.05	.769	.730	.716	.717	.628	.506	.512	.509

Table 1 (Continued).

RSB B	SNR spec	Terra				Aqua			
		PL	2000	2008	2011	PL	2002	2008	2011
33	0.25	.556	.528	.522	.524	.308	.321	.323	.325
34	0.25	.793	.791	.775	.778	.482	.477	.480	.484
35	0.25	.978	.942	.930	.933	.539	.598	.601	.606
36	0.35	1.29	1.27	1.24	1.25	.725	.647	.651	.656

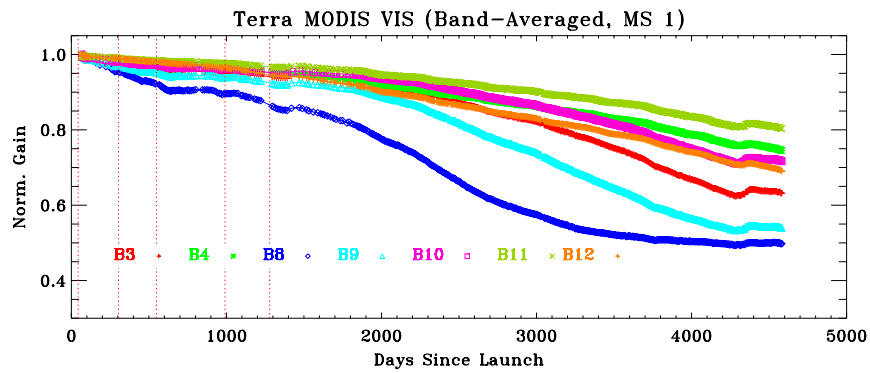


Fig. 1 Terra MODIS VIS band gain trending for MS1.

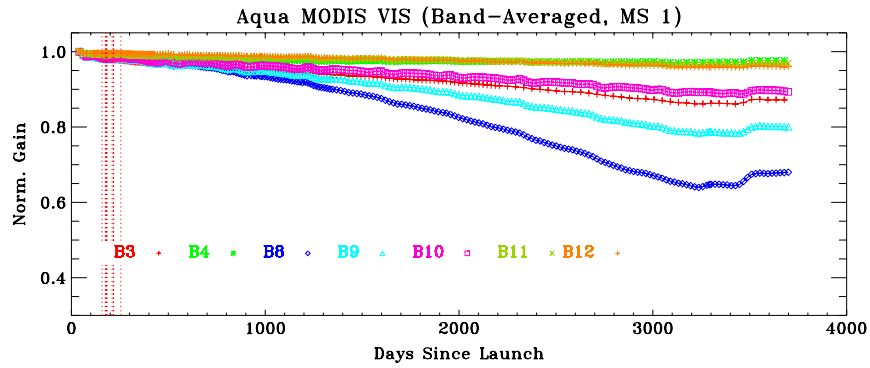


Fig. 2 Aqua MODIS VIS band gain trending for MS1.

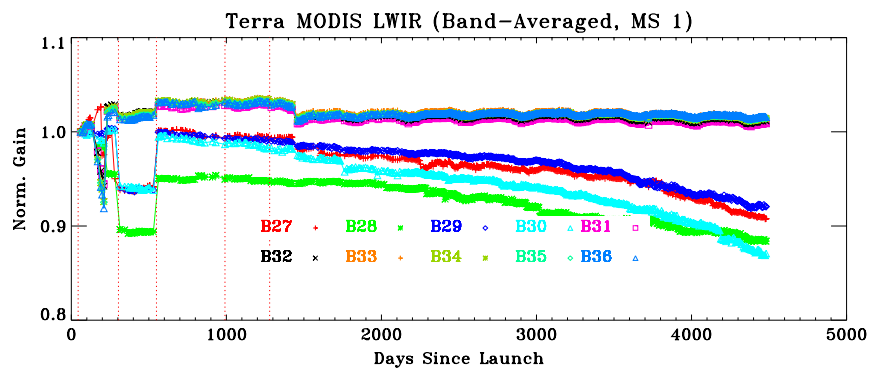


Fig. 3 Terra MODIS long-term stability for TEB LWIR FPA, MS1.

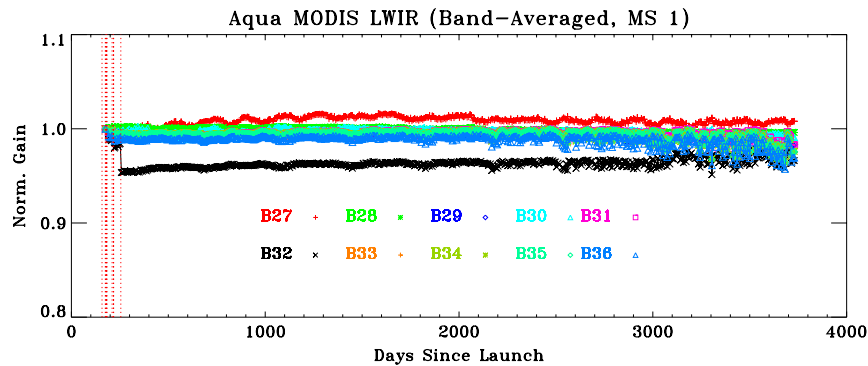


Fig. 4 Aqua MODIS long-term stability for TEB LWIR FPA, MS1.

Radiometric stability for the TEB is assessed by trending the linear gain coefficient b_1 , which is measured at every scan. As an example, the plot in Fig. 3 displays Terra long-term stability for MS1 observations from the LWIR FPA. The corresponding Aqua data is provided in Fig. 4. In both figures, the data for each band are averaged over all operational detectors, excluding noisy detectors. Major changes correlate with the occurrence of key operational events.³ The increase in gain fluctuations seen in certain Aqua LWIR bands in the last few years is due to the increasing difficulty of maintaining a constant temperature on the cold FPA where the LWIR sensors are housed. Terra RSB gain was affected by the SD door failure in 2003. Further calibration and performance information is available.¹⁰

4 L1B Data Products and Development

The MODIS L1B algorithms generate radiometrically calibrated L1B science data sets (SDS). The L1B software ingests geo-located data, performs QA, calibrates all detectors, transforms raw data numbers (DN) into radiance and reflectance, converts engineering counts into engineering units, produces the L1B data products, creates metadata, and appends metadata. The algorithms are based on the MODIS Algorithm Theoretical Basis Document.¹⁹

L1B software produces three files containing EV data obtained at the MODIS spatial resolutions of 1 km/pixel, 500 m/pixel, and 250 m/pixel. Scientific EV data are stored in HDF-4 format as 16-bit unsigned integer SDS, referred to as scaled integer SDS. A set of band-dependent scale and offset terms provided in the L1B output as SDS attributes allow the conversion of the TEB SDS to radiance and the RSB SDS to radiance and reflectance for each pixel. The MODIS L1B Product User's Guide²⁰ describes this process.

Data quality flags are assigned to each scan. The performance of the 490 detectors on each MODIS instrument is tracked daily and expressed in a time-dependent detector QA LUT.³ An SDS denoting uncertainty level consisting of an unsigned integer from 0 to 15, with 0 indicating the lowest uncertainty, is also generated for each scaled integer SDS. SDS attributes are used to convert these values into percentage uncertainty. L1B also produces on-board calibrator data products, containing the raw SV dn , averaged SV dn , SD data, SRCA data, BB data, and all telemetry used for calibration. These data are principally used by MCST. The principal MODIS L1B EV Science Data Products²⁰ and detailed file descriptions²¹ are available through the Level 1 and Atmospheres Archive and Distribution System (LAADS).²² The search may be filtered by time, the area covered, Day/Night/Both, PGEVersion, and QAPercentMissingData.

The L1B code and LUT histories, calibration information, instrument operation activities, and related documentation are available at the MCST website.¹⁰ Development milestones are presented in Table 2. Postlaunch L1B revisions derive from many sources, among them the discovery of software bugs; upgrades to the reliability, efficiency, or portability of the code; and modifications based on improved characterization of the MODIS instruments based on analysis of in-orbit data. When a significant change to L1B is proposed, the science team, representing the atmosphere, land, and ocean disciplines, in consultation with MCST considers the impact on the data products and data quality. The science team decides whether to implement changes, begin processing current data as a new collection, and reprocess previous data with the

Table 2 L1B algorithm development milestones.

L1B milestone	Date
Start coding	1993
Software requirements review	March 1995
Preliminary design review for version 1	June 1995
Critical design review for version 1	December 1995
Version 1 delivery (all major functions, interfaces, messages)	March 1996
Preliminary design review for version 2	September 1996
Critical design review for version 2	December 1996
Version 2 Terra launch-ready delivery	February 1997
Re-delivery of version 2 (L1A and geo-location compatible)	September 1997
Prelaunch code version 2.1.3	March 1999
Terra postlaunch code version 2.3.2 (collection 2)	March 2000
Terra code version 3 (collection 3)	May 2001
Aqua code version 3 (launch-ready collection 3)	April 2002
Aqua code version 4 (collection 4)	October 2002
Terra code version 4 (collection 4)	January 2003
Terra code version 5 (collection 5)	March 2005
Aqua code version 5 (collection 5)	July 2005
Aqua code version 6 (collection 6)	January 2012
Terra code version 6 (collection 6)	August 2012

new L1B version to produce long-term data product consistency. Within each collection, the accuracy of the data products is maintained by updating the Terra and Aqua LUTs that provide the MODIS characterization to the L1B code.²³ These tables also provide updates that account for changes in sensor performance. Recently, based on the improvements discussed in Sec. 5, Terra and Aqua MODIS have implemented collection 6 processing. In C6, there are 107 Terra LUTs and 111 Aqua LUTs.

The Terra and Aqua collection history prior to collection 5 and the improvements to the initial collection 5 algorithm have been previously presented.³ Continuing beyond the time period described in Toller et al.,³ Table 3 describes more recent Terra and Aqua/MODIS L1B collection 5 code improvements that are also included in C6. The information is provided individually for Terra and Aqua MODIS in time order.

The annual rate of L1B and LUT deliveries for collections C2 through C5 from 2000 through 2006, excluding internal MCST deliveries and special deliveries to the Ocean Color, University of Miami, and University of Wisconsin groups, was previously presented.³ From 2007 to the end of 2012, six new Terra code versions were released, as well as 102 C5 LUT updates and 7 C6 LUT updates. In that time, five new Aqua code versions were released, along with 67 C5 LUT updates and 11 C6 LUT updates.

5 Improvements for Collection 6 Processing

Currently, to mitigate instrumental effects, MODIS has initiated C6 processing, which includes reprocessing of all data from the beginning of the Terra and Aqua missions. C6 enhancements are

Table 3 Terra and Aqua MODIS collection 5 L1B code changes.

Terra code version	Production start data day	Description of L1B code upgrades
5.0.6	3/7/2005	New LUT-enabled band 21 calibration with mirror-side dependence; new LUT-enabled SWIR out-of-band correction detector dependence; corrected dimension mapping offset setting for 250-meter resolution band data; improved code portability
5.0.38	9/17/2007	RVS correction limit range extended
5.0.40	1/24/2008	Based the metadata version on the MODAPS PGE version in lieu of the obsolete GDAAC PGE version
5.0.42	7/10/2009	Added. NRT identifier to LOCALGRANULEID metadata to identify "near real time" production
5.0.44	8/23/2009	Only the PGE02 version changed for a correction to a PGE level error
5.0.46	5/16/2010	Fixed the sector rotation issue that can produce artificially high TEB radiances for a number of scans before the instrument performs a sector rotation for lunar data acquisition

Aqua code version	Production start data day	Description of IL1B code upgrades
5.0.7	7/3/2005	New LUT-enabled band 21 calibration with mirror-side dependence; new LUT-enabled SWIR out-of-band correction detector dependence; corrected dimension mapping offset setting for 250-meter resolution band data; improved code portability
5.0.35	1/23/2008	RVS correction limit range extended; based the metadata version on the MODAPS PGE version in lieu of the obsolete GDAAC PGE version
5.0.37	7/10/2009	Added. NRT identifier to LOCALGRANULEID metadata to identify "near real time" production
5.0.39	5/12/2010	Fixed the sector rotation issue that can produce artificially high TEB radiances for a number of scans before the instrument performs a sector rotation for lunar data acquisition
5.0.41	4/5/2012	Improved default b_1 calculation

generated in response to improved instrument characterization methodologies and feedback from the scientific community.²⁴ The MODIS characterization is achieved through data analysis, which includes data trending, ongoing calibration of all operational detectors, special studies of operational anomalies, comparison between Terra and Aqua, comparison with other missions, ground truth studies, and regular communication with the science team. The improvements are implemented through numerous L1B LUT updates. Occasionally, the addition of a new LUT or a code modification becomes necessary. These upgrades can vary between the two MODIS instruments.

Aqua C6 L1B data production began in January 2012. Reprocessing of all prior Aqua data was completed by the end of March 2012. Aqua C6 is now being applied to current data (called forward processing). Terra L1B reprocessing started in August 2012 and finished in October 2012.

Changes implemented for C6 processing are listed in Table 4. A few of these changes were implemented near the end of C5 but were not applied to all mission data. Improvements in ocean color band products (bands 8 to 16), aerosol products (bands 1 to 4), and temperature retrievals are expected. The most significant of the improvements listed in Table 4 are discussed in more detail below.

5.1 Handling Missing Data

In C5 and all previous collections, pixels containing data collected from an inoperable detector were filled in by linear interpolation from nearby good detectors. In C6, at the request of the

Table 4 Terra and Aqua MODIS changes for collection 6.

Nature of the change	Description of upgrades for both Terra and Aqua
Code	New treatment of data from inoperable detector
Code	Fixed the sector rotation issue
Code	Addressed PCLW electronics issue
LUT	RSB correction for SDSM D9 degradation
LUT	New m_1 tables (includes SDSM D9 degradation correction)
LUT	Using EV data at several AOI and lunar data to derive m_1 and RVS for Terra bands 1 to 4, 8, and 9 and Aqua bands 8 to 9
LUT	Time-dependent RVS for bands 13 to 16
LUT	Detector-dependent RVS for in bands 8 to 12 (plus Terra band 3)
Code, LUT	RVS fit using a fourth-order polynomial
LUT	Modified derivation of TEB offset and nonlinear calibration coefficients
Code	New computation of the uncertainty index (UI)
New LUTs	Added six RSB and 11 TEB LUTs for improved uncertainty determination
Remove LUTs	Eight RSB and five TEB LUTs no longer needed by new uncertainty algorithm
Code, New LUT	Quality assurance flags expanded from a detector basis to a subframe basis
Output	Added a product file attribute that indicates noisy subframes
Output	Added a noisy subframe list
Output	Added a dead subframe list
Output	Added a product file attribute that indicates pixels affected by dead subframes
Nature of the change	Description of other Terra upgrades
LUT	Time-dependent RVS for bands 17 to 19
Nature of the change	Description of other Aqua upgrades
LUT	Treatment of MS2 RVS
Code, new LUTs	New calibration treatment during WUCD band 33, 35, and 36 saturation. Added three new LUTs for determining default band 33, 35, and 36 b_1 values
LUT	Modified derivation of a_0 and a_2 coefficients to account for cold FPA fluctuations

science team, such pixels are filled in with a specific flag value. In neither collection are such pixels used when aggregating values to lower resolution. This change provides purer, less manipulated data but results in image stripes that readily show that a detector is inoperable. Users can apply postprocessing code to generate the image data with interpolation.

5.2 SD Degradation

A significant RSB change includes a correction for long-term degradation of SDSM detector 9 (D9). In C5, the SD degradation was derived using the SD/Sun ratios and normalizing to the response of SDSM D9. Although D9 degradation is very small near the beginning of the mission, there is a cumulative effect. The impact of the long-term degradation of SDSM D9 (currently 2% for Terra MODIS and 0.6% for Aqua MODIS) is corrected in the C6 LUTs for both Terra and Aqua MODIS. A similar correction was initiated in the C5 LUTs with a smooth transitioning over a period of three months in order to avoid sudden changes in the L1B products. Using the

refitted SD degradation and SDSM D9 correction, the m_1 calibration tables were recalculated and fit using multiple fitting segments to generate the final C6 m_1 LUTs over the entire mission. Time steps were added to handle instrument configuration changes.

5.3 RSB Response Versus Scan Angle

The dependence of the MODIS scan mirror's response as a function of the AOI is described by the RVS, which was characterized prelaunch for both Terra and Aqua MODIS. Since the difference in the PL RVS among detectors of each band²⁵ was less than 0.13%, the PL RVS was obtained by averaging over all detectors for each MS of a band. In orbit, the time-dependent RVS change is wavelength dependent, with more change seen at the shorter wavelengths. Studies of RVS change have improved the C6 EV measurements.²⁶

Time-dependent RVS LUTs have been applied to selected bands in MODIS L1B since collection 4 for both instruments. In C5, band-averaged responses from the SD and lunar measurements were applied to compute the Aqua RSB RVS and the Terra MS1 RVS. For Terra RSB MS2, the C5 RVS was created using the response ratios between the two MSs, derived using Earth-view observations, lunar measurements, and on-board calibrators with MS1 as a reference. In C6, the Terra RSB RVS approach used in C5 was extended to both Aqua and Terra for most RSBs. In other words, EV, SRCA, SD, and lunar response MS ratios were also used to derive Aqua MS2 RVS using MS1 RVS as a reference.

Application of a detector-dependent RVS for Terra MODIS bands 3 and 8 to 12 and Aqua bands 8 to 12 is one of the major improvements in C6. A detector-dependent RVS mitigates the detector-to-detector differences observed in the calibrated EV images, thereby reducing striping.²⁵ As an example, Fig. 5 provides the detector-to-detector percentage differences (detector response relative to the average of all good detectors) versus time (beginning with 1/1/2000) for C5 (left panel) and C6 (right panel). The different colors denote the different detectors for the band. This comparison shows the striping reduction achieved in C6 for the 10 detectors of Terra band 8, MS1, at the AOI of the moon. For Aqua MODIS VIS bands, the detector-to-detector differences are also mitigated in C6, although the improvement is not as dramatic, because the detector bias was generally less than 1% in C5.

In C5 and earlier collections, a time-dependent gain from the SD and the PL RVS were used to generate the L1B products for bands 13 to 16. Intensive studies of the in-orbit RVS change determined the need to update the RVS LUTs by applying a time-dependent RVS for these bands in C6. Because the lunar measurements needed to derive the time-dependent RVS for these high-gain ocean bands are partially saturated, MCST developed a ratio approach using lunar measurements from unsaturated bands to derive the long-term lunar trending. For Terra bands 17 to 19, a time-dependent RVS was incorporated in the latter C5 timeframe and subsequently applied to all C6 processing.

A C6 innovation is the development and implementation of an alternative approach to derive m_1 and RVS using EV data from time-invariant desert sites at several AOIs to supplement the on-board measurements from the SD and moon. This method is applied to Terra bands 1 to 4, 8, and 9 and Aqua bands 8 and 9 in C6. The Terra RVS fit uses a second-order polynomial for bands 1

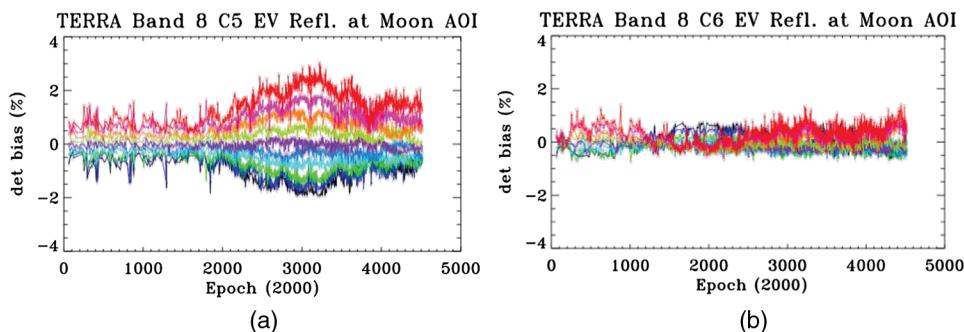


Fig. 5 Striping comparison between C5 (a) and C6 (b) for Terra EV band 8, MS1 radiance at the lunar AOI.

and 2 and a fourth-order polynomial fit using EV dn obtained at 13 selected AOIs for bands 3, 4, 8, and 9 for each MS. The Aqua C6 RVS fit uses a fourth-order polynomial for each MS of bands 8 and 9 over a dozen selected AOIs. The new polynomial required a LUT change, while the evaluation of the polynomial as a function of AOI necessitated a code change. The inverse of the polynomial at the AOI of the SD is the detector-averaged m_1 in-orbit variation. Normalizing the polynomial by this m_1 provides the detector-averaged RVS in-orbit variation. Applying the alternative approach produces an improved in-orbit RVS and significantly mitigates the long-term drifts observed in these bands. This improvement in the radiometric product signifies the alternative approach as the major RSB achievement in C6.

Based on the RSB improvements described in this section, MCST has studied the expected Terra and Aqua C6 to C5 reflectance ratios based on test data from the years 2006 and 2012. Results indicate the maximum difference resulting from C6 improvements is a 10.2% increase in the Terra C6/C5 reflectance ratio²⁶ in band 8. The corresponding value for Aqua is 3.8%, also in band 8. The percentage difference is both time and AOI dependent. The more precise C6 reflectances improve the EV data quality and significantly mitigate the long-term drift, especially in the short-wavelength bands.

The effect of the band 8 improvement should be most noticeable in the ocean and aerosol products. The median of the reflectance ratios for all RSBs at the AOI of the SV, nadir, and SD is 1.001 for Terra and 0.997 for Aqua. The standard deviation from these median ratio values is greater for Terra than for Aqua.

5.4 TEB Calibration Coefficients

The most important TEB modification entails the methodology to derive the offset (a_0) and nonlinear (a_2) calibration coefficients. For Terra, the current electronics/formatter configuration necessitates the use of coefficients derived from the in-orbit BB WUCD data. Band 21, a low-gain fire detection band, is treated separately and has a_0 and a_2 set to 0. In contrast to C5, where all other TEB a_0 and a_2 coefficients are derived from BB warmup data (except bands 33 to 36, which have a_0 set equal to 0), Terra C6 sets a_0 to 0 for all MS1 TEBs. The MS2 coefficients for bands 20, 22 to 25, and 27 to 30 have a slight offset from 0 to account for the relative difference between the two MSs. This mirror-side difference is derived from the WUCD activities. Comparison of simultaneous nadir observations between Terra MODIS and the infrared atmospheric sounding interferometer (IASI) instrument provided independent confirmation of the C6 a_0 approach.²⁷ Regular observations of the Dome C, Antarctica region allowed tracking of the consistency between Terra and Aqua TEB retrievals.²⁸ These comparisons, supported by studies relating Aqua MODIS to the atmospheric infrared sounder (AIRS),²⁹ led MCST to conclude that Terra MODIS TEB temperature retrievals were too warm at very cold scene temperatures. Using C6 processing produces a significant improvement in the cold scene Terra: IASI and Terra: Aqua comparisons.³⁰ Another change is that Terra and Aqua a_2 coefficients are derived from the BB cooldown data in C6. This approach is believed to provide improved accuracy due to the passive cooldown process and a more gradual rate of temperature change of the BB during the cooldown cycle compared with the active control process during the warmup cycle.

For Aqua, the PL-derived coefficients have been generally adequate to date for all bands except 31 and 32. A gain change for bands 31 and 32 requires the use of in-orbit-derived coefficients. In C6, for Aqua bands 31 and 32, a_0 is set to 0, and a_2 is derived from BB cooldown data. An additional influence on Aqua TEB calibration exists because of drift of the SMIR and LWIR FPA temperatures from their nominal setting of 83 K. Due to a slow loss of radiative cooler margin in recent years, the FPA temperature undergoes orbital and seasonal oscillations.³¹ A modified algorithm was derived to compensate for SMIR and LWIR FPA temperature fluctuations during the WUCD analysis. This upgrade, implemented as a forward update on July 3, 2012, led to greater consistency with Aqua PL a_2 , particularly for bands 33 to 36. Any observed in-orbit relative drift as derived from the WUCD activities is applied as an adjustment to the PL a_2 values.

For both Terra and Aqua MODIS, the a_0 and a_2 coefficients derived from the quarterly in-orbit WUCD activities are monitored regularly, and updated LUTs are delivered as needed. Additionally, a new Aqua default b_1 TEB LUT compensates for LWIR FPA temperature

Table 5 Expected C6-C5 TEB temperature retrieval differences (K).

Band	T_{typ}	Terra			Aqua		
		ΔT at. $3L_{\text{typ}}$	ΔT at. L_{typ}	ΔT at. $9L_{\text{max}}$	ΔT at. $3L_{\text{typ}}$	ΔT at. L_{typ}	ΔT at. $9L_{\text{max}}$
20	300	-0.20	+0.02	-0.30	0.00	0.00	-0.03
22	300	-0.20	+0.02	-0.20	0.00	0.00	0.00
23	300	-0.20	+0.02	-0.20	0.00	0.00	-0.01
24	250	-4.50	-1.00	-0.50	0.00	0.00	0.00
25	275	-1.00	-0.15	-0.07	0.00	0.00	0.00
27	240	-5.00	-1.35	-0.25	-0.02	-0.02	-0.01
28	250	-5.50	-1.00	-0.25	-0.01	-0.01	-0.01
29	300	-1.00	-0.03	-0.30	-0.05	0.04	0.13
30	250	-9.50	-1.60	-0.40	-0.13	-0.11	-0.05
31	300	-0.20	-0.04	-0.13	-0.40	0.00	-0.05
32	300	-0.20	-0.04	-0.14	-0.40	0.00	-0.05
33	260	+0.10	+0.06	+0.02	+0.01	0.00	0.00
34	250	+0.10	+0.06	+0.05	0.00	0.00	0.00
35	240	+0.10	+0.06	+0.05	-0.12	-0.10	-0.07
36	220	+0.05	+0.02	+0.02	+0.02	+0.02	+0.02

variation during WUCD in lieu of the previously constant default b_1 value, resulting in a more accurate b_1 determination. This treatment is applied only for Aqua bands 33, 35, and 36, since these bands saturate at the higher BB temperatures encountered during the WUCD. The magnitude of this change on the EV temperature during periods when the BB temperature exceeds the saturation temperature is less than 0.1 K early in the Aqua mission but reaches as much as ± 2 K in 2012. Implementing the calibration of bands 33, 35, and 36 during WUCD also required a new Aqua algorithm that calculates the default b_1 value. This upgrade was delivered in July 2011 as a C5 forward processing update and is applied to all mission data in C6.

Table 5 (where L_{max} is the maximum radiance, L_{typ} is the typical radiance) shows test case results for the quantitative temperature retrieval differences at three radiance levels as a result of implementing this new methodology. Actual differences are detector and time dependent. Temperature retrieval differences for fire band 21 are generally within ± 2 K.

5.5 Other Modifications

During lunar measurements, MODIS performs a sector rotation that alters the starting point of a scan. This causes an occasional discrepancy between the actual and reported starting scans of the sector rotation in the L1B data. As a consequence, artificially high TEB radiances may be produced for 40 scans before the start of the lunar measurement. To correct this, a code change was introduced late in C5 and was applied only to Terra and Aqua MODIS forward processing. The same fix was applied to C6 and is being used for both forward and reprocessed data.

A code change for C6 handles the case in which the long-wavelength photoconductive electronics side A and side B are both commanded on at the same time. Previously, this command, which is incompatible with the current hardware configuration, would have led to the loss of a 5-min granule. The C6 code marks the affected 1.48-s scan as bad.

L1B C6 has resulted in improved uncertainty index (UI) assessment for each pixel. The Terra and Aqua TEB UI now includes the offset (a_0) and nonlinear (a_2) calibration coefficient

uncertainty. A few PL uncertainty terms have been replaced with values based on EV observations. The improved C6 in-orbit RVS characterization algorithm successfully addressed the long-term drifts seen in the short-wavelength VIS band responses. Also, the RVS uncertainty at the EV and SD AOI now depend on whether the RVS is normalized to the SD AOI (EV measurements) or the SV AOI (lunar observations). Three C6 RSB uncertainty terms are provided by time-dependent LUTs, while two other terms are scene dependent and therefore calculated based on LUT parameters. The improved UI assessment does not always result in decreased uncertainty values.

Bands 1 and 2 have four subframes, and bands 3 to 7 have two subframes. The revised QA LUT provides subframe-level QA flags. Previous collections had QA flags applied only on a detector basis. The new LUT allows noisy subframes to be flagged. Therefore, L1B product files contain an HDF-4 file attribute named “Detector Quality Flag2,” which contains a bit-mask for each high-resolution detector indicating which subframes are noisy. There is also a “Noisy Subframe List” that contains one byte for every subframe for every high-resolution detector, with a value of 1 indicating a noisy subframe. Anticipating that, at some future time, the noise might justify marking a particular subframe as inoperable, MCST added an HDF file attribute named “Dead Subframe List”(currently empty) and corresponding bit flags in Detector Quality Flag2. If this case occurs, pixels containing data affected by this problem will be filled with a value of 65,525. For each high-resolution detector, the percentage of Earth-view pixels affected by dead subframes is available in a new HDF file attribute named “% Dead Subframe EV Data.”

Numerous LUT changes were made in preparation for C6 processing. These included updating the time-dependent designations of detectors as being noisy, out of family, or inoperable. Also, the BB temperature at which the L1B algorithm switches to the default linear calibration coefficient b_1 for the case when Aqua bands 33, 35, and 36 saturate during WUCD was increased, allowing more data to be calibrated with the scan-by-scan coefficients. Another LUT change was needed to achieve compatibility with the UI code change.

6 Lessons Learned

MCST has gained invaluable experience in all phases of NASA EOS missions during the 13 years since the launch of Terra and the beginning of the MODIS data collection era. The Aqua mission has provided nearly as long an opportunity to glean valuable lessons for future missions. First, a dedicated calibration team is essential to maintain a consistently high science data quality over the instrument lifetime. Second, continuity in the calibration team allows for the retention and transfer of historical knowledge from the PL phase to in-orbit operations. Third, a dedicated calibration team facilitates the acquisition of technical expertise to address the challenging issues that inevitably arise during the mission.

Both MODIS instruments continue to operate well beyond their designed prime lifetime of 6 years. The sustained calibration effort includes routine tracking of instrument performance and the flexibility to modify and update the methodology and algorithms as new information is gathered. This results in improved versions of the entire MODIS data set delivered by the calibration team, even as the instrument changes with age and use. Collection 6 development benefited from a close collaboration of the calibration team with representatives of the MODIS science team. Regular bi-weekly meetings of the MODIS sensor Working Group (MsWG) are a forum for discussion of instrument issues, concerns, and proposed changes to operational algorithms. The science discipline representatives who attend the MsWG meetings provide useful feedback to the calibration team from the science product perspective. This allows all calibration modifications to be thoroughly vetted and the potential impact on downstream products to be assessed. Understanding the impact of L1B code and LUT changes on the Level-2 and Level-3 products is imperative for science data record continuity and consistency.

7 Conclusion

Terra and Aqua MODIS have successfully provided global observations of the Earth’s land, oceans, and atmosphere for more than a decade. The two MODIS instruments are nearly

identical, allowing a common calibration approach. Improvements have been made to the L1B algorithm in preparation for collection 6 processing as in-orbit data analysis led to improved instrument characterization.

The sustained instrument calibration and characterization program has enabled upgrades to the L1B algorithm, resulting in the delivery of well-calibrated scientific data products that continue to meet mission specifications after more than a decade of in-orbit operations. The L1B improvements in each collection are implemented via numerous L1B LUTs and occasional code changes that can vary between the two MODIS instruments. Calibration and instrument characterization are described on the MCST website.¹⁰ The changes to the latest (C6) version of L1B have been presented, and the expected consequences have been described in terms of reflectance ratios, striping, Terra: Aqua comparison, and temperature retrieval differences.

Challenges remain as the instruments age and degrade. However, QA trending and data analysis results support the expectation that the MODIS instruments will continue to add high-quality data to the long-term climate data record.

Acknowledgments

Marghi Hopkins supported the initial L1B code design. Subsequent versions of L1B leading to the first operational code were developed by Jim Rogers. Alice Isaacman incorporated later L1B upgrades. The authors would also like to thank present and former members of the MCST for their expertise. Additionally, several members of the MODIS Science Team provided advice, data analysis, and algorithms, which resulted in substantial improvements to the L1B code.

References

1. V. Salomonson, B. Guenther, and E. Masuoka, "A summary of the status of the EOS terra mission moderate resolution imaging spectroradiometer (MODIS) and attendant data product development after one year of on-orbit performance," in *Proc. Int. Geosci. Rem. Sens. Symp./IGARSS*, Vol. 3, pp. 1197–1199, IEEE, Sidney, Australia (2001).
2. W. L. Barnes, T.S. Pagano, and V.V. Salomonson, "Pre-launch characteristics of the moderate resolution imaging spectroradiometer (MODIS) on EOS-AM1," *IEEE Trans. Geosci. Rem. Sens.* **36**(4), 1088–1100 (1998), <http://dx.doi.org/10.1109/36.700993>.
3. G. Toller et al., "Status of earth observing system terra and aqua MODIS Level 1B algorithm," *J. Appl. Rem. Sens.* **2**(1), 023505 (2008), <http://dx.doi.org/10.1117/1.2839442>.
4. A. Isaacman et al., "MODIS level 1B calibration and data products," *Proc. SPIE* **5151**, 552–562 (2003), <http://dx.doi.org/10.1117/12.507957>.
5. X. Xiong, A. Isaacman, and W. Barnes, "MODIS Level 1B products," in *Earth Science Satellite Remote Sensing*, J. J. Qu et al., Eds., Vol. 1, pp. 33–49, Tsinghua University Press and Springer-Verlag, New York (2006).
6. X. Xiong et al., "Status of MODIS Level 1B algorithms and calibration tables," in *Proc. IEEE Int. Geosci. Rem. Sens. Symp.*, Vol. 3, pp. 2231–2234, IEEE, Seoul, Korea (2005).
7. X. Xiong, B. Wenny, and W. Barnes, "Overview of NASA Earth observing systems Terra and Aqua moderate resolution imaging spectroradiometer instrument calibration algorithms and on-orbit performance," *J. Appl. Rem. Sens.* **3**(1), 032501 (2009) <http://dx.doi.org/10.1117/1.3180864>.
8. X. Xiong and W. Barnes, "MODIS calibration and characterization," in *Earth Science Satellite Remote Sensing*, J.J. Qu et al., Eds., Vol. 2, pp. 77–97, Tsinghua University Press and Springer-Verlag, New York (2006).
9. V. Salomonson, W. Barnes, and E. Masuoka, "Introduction to MODIS and an overview of associated activities," in *Earth Science Satellite Remote Sensing*, J. J. Qu et al., Eds., Vol. 1, pp. 13–32, Tsinghua University Press and Springer-Verlag, New York (2006).
10. MODIS Characterization Support Team (MCST), NASA Goddard Space Flight Center, <http://mcst.gsfc.nasa.gov/> (21 September 2012).
11. X. Xiong et al., "MODIS on-board blackbody function and performance," *IEEE Trans. Geosci. Rem. Sens.* **47**(10) (2009), <http://dx.doi.org/10.1109/TGRS.2009.2023317>.

12. X. Xiong et al., “Multiyear on-orbit calibration and performance of Terra MODIS thermal emissive bands,” *IEEE Trans. Geosci. Rem. Sens.* **46**(6), 1790–1803 (2008), <http://dx.doi.org/10.1109/TGRS.2008.916217>.
13. X. Xiong, N. Che, and W. Barnes, “Terra MODIS on-orbit spatial characterization and performance,” *IEEE Trans. Geosci. Rem. Sens.* **43**(2), 355–365 (2005), <http://dx.doi.org/10.1109/TGRS.2004.840643>.
14. X. Xiong, N. Che, and W. Barnes, “Terra MODIS on-orbit spectral characterization and performance,” *IEEE Trans. Geosci. Rem. Sens.* **44**(8), 2198–2206 (2006), <http://dx.doi.org/10.1109/TGRS.2006.872083>.
15. X. Xiong et al., “On-orbit calibration and performance of Aqua MODIS reflective solar bands,” *IEEE Trans. Geosci. Rem. Sens.* **48**(1), 535–546 (2010) <http://dx.doi.org/10.1109/TGRS.2009.2024307>.
16. X. Xiong et al., “Multiyear on-orbit calibration and performance of Terra MODIS reflective solar bands,” *IEEE Trans. Geosci. Rem. Sens.* **45**(4), 879–889 (2007), <http://dx.doi.org/10.1109/TGRS.2006.890567>.
17. J. Sun et al., “MODIS reflective solar bands on-orbit Lunar calibration,” *IEEE Trans. Geosci. Rem. Sens.* **45**, 2383–2393 (2007), <http://dx.doi.org/10.1109/TGRS.2007.896541>.
18. X. Xiong et al., “MODIS thermal emissive bands calibration algorithm and on-orbit performance,” *Proc. SPIE*, **4891**, 392–401 (2002), <http://dx.doi.org/10.1117/12.466083>.
19. J. Xiong et al., “MODIS Level 1B algorithm theoretical basis document, Version 3,” NASA Goddard Space Flight Center, Greenbelt, MD, http://mcst.gsfc.nasa.gov/sites/mcst.gsfc/files/file_attachments/M1058.pdf (21 September 2012).
20. MODIS Characterization Support Team., “MODIS Level 1B Product User’s Guide- For Level 1B Version 6.1.014 (Terra) and Version 6.1.17 (Aqua),” MCM-PUB-01-U-0202-Rev D, <http://mcst.gsfc.nasa.gov/11b/documents> (21 September 2012).
21. MODIS Characterization Support Team., “MODIS Level 1B Products Data Dictionary- Applicable to Level 1B code Version 6.1.14, file specifications Version 6.1.14. (MODIS/ Terra) and to Level 1B code Version 6.1.17, file specifications Version 6.1.17 (MODIS/ Aqua),” MCM-02-2.3.1-PROC-L1BPDD-U-01-0107-REV D, <http://mcst.gsfc.nasa.gov/11b/documents> (21 September 2012).
22. Science Data Support Team, NASA Goddard Space Flight Center, <http://ladsweb.nascom.nasa.gov> (21 September 2012).
23. MODIS Characterization Support Team, Goddard NASA Space Flight Center, “MODIS LUT Information Guide for Level 1B Version 6.1.14 (Terra) and Version 6.1.17 (Aqua) (2012),” <http://mcst.gsfc.nasa.gov/11b/documents> (21 September 2012).
24. B. Wenny et al., “MODIS calibration algorithm improvements developed for collection 6 Level-1B,” *Proc. SPIE* **7807**, 78071F (2010), <http://dx.doi.org/10.1117/12.860892>.
25. J. Sun et al., “Time-dependent response versus scan angle and its uncertainty for MODIS reflective solar bands,” *Proc. SPIE* **7826**, 782620 (2010), <http://dx.doi.org/10.1117/12.864735>.
26. J. Sun et al., “Time-dependent response versus scan angle for MODIS reflective solar bands,” *Proc. SPIE* **7452**, 745219 (2009), <http://dx.doi.org/10.1117/12.825168>.
27. C. Moeller et al., “Revisiting IASI-MODIS TEB Comparisons,” MODIS Science Team Meeting, MCST Calibration Workshop, May 9, 2012, http://mcst.gsfc.nasa.gov/sites/mcst.gsfc/files/meetings_files/STM2012_Cal_Moeller.pdf (21 September 2012).
28. X. Xiong, A. Wu, and B. Wenny, “Using Dome C for moderate resolution imaging spectroradiometer calibration stability and consistency,” *J. Appl. Rem. Sens.* **3**(1), 033520 (2009), <http://dx.doi.org/10.1117/1.3116663>.
29. D. Tobin et al., “Use of atmospheric infrared sounder high-spectral resolution spectra to assess the calibration of moderate resolution imaging spectroradiometer on EOS Aqua,” *J. Geophys. Res.* **111**, D09S05 (2006), <http://dx.doi.org/10.1029/2005JD006095>.
30. Y. Li, A. Wu, and X. Xiong, “Evaluating calibration of MODIS thermal emissive bands using infrared atmospheric sounding interferometer measurements,” **8724**, in press (2013).
31. Z. Wang et al., “Monitoring and assessment of the temperature fluctuation of Aqua MODIS cold focal plane assembly,” *Proc. SPIE* **8510**, 85100K (2012), <http://dx.doi.org/10.1117/12.930904>.



Gary Toller is a senior scientist at Sigma Space Corp., in Lanham MD. After receiving a BS degree in physics and mathematics from Dickinson College and PhD in astronomy from SUNY Stony Brook, he has supported remote sensing projects for more than 30 years. Currently, he is a member of the MODIS Characterization Support Team. Previously he supported NASA's Cosmic Background Explorer (COBE) Mission, the Tropical Rainfall Measurement Mission (TRMM), the Advanced Earth Observing Satellite-II (ADEOS-II), Space Transportation System (space shuttle STS-3), and Pioneer 10 and 11 space probes. He also teaches in the McDaniel College physics department.



Xiaoxiong Xiong is an optical physicist at NASA Goddard Space Flight Center (GSFC), working on the EOS and NPOESS Preparatory Project (NPP) sensor calibration and characterization. He is currently serving as the MODIS Project Scientist for the instrument operation and calibration and the technical lead for both the MODIS Characterization Support Team (MCST) and the NPP Instrument Calibration Support Team (NICST). He received a BS degree in optical engineering from Beijing Institute of Technology, Beijing, China and a PhD in physics from University of Maryland, College Park, Maryland. Before joining the NASA/GSFC, he had also worked in the fields of optical instrumentation, nonlinear optics, laser / atomic spectroscopy, and mass spectrometry at private industry and at National Institute of Standards and Technology (NIST).



Junqiang Sun is a chief support scientist at Sigma Space Corp. in Lanham, MD, serving as technical leader for the MODIS Characterization Support Team (MCST) and also works on NPOESS/VIIRS instrument calibration and characterization. He received a BS in physics from Changsha Institute of Technology, Changsha, China, a physics PhD from University of Science and Technology of China, Hefei, China, and a PhD in chemistry from University of Florida, Gainesville, Florida. Before joining Sigma Space Corp., he was a lead scientist at Science Systems and Applications, Inc. and worked on MODIS and VIIRS calibration and characterization. He has also worked extensively in atomic and molecular physics at Freie Universitaet Berlin and the University of Kansas and in quantum chemistry at Iowa State University and the University of Florida.



Brian N. Wenny received a BS degree in physics from Ursinus College in Collegeville, PA in 1991, and MS and PhD degrees in atmospheric science from North Carolina State University, Raleigh, in 1996 and 2000, respectively. He is currently a senior scientist and calibration team leader with the MODIS Characterization Support Team (MCST) at Sigma Space Corp. in Lanham, MD. Before joining MCST, he was a scientist with Science Applications International Corporation in support of the Stratospheric Aerosol and Gas Experiment III (SAGE III) at NASA Langley Research Center.

Xu Geng received a BS degree in engineering mechanics from TsingHua University, Beijing, China, and a PhD degree in mechanical engineering from Johns Hopkins University. He is currently working on the instrument calibration and data analysis with the MODIS Characterization Support Team (MCST).



Amit Angal received a MS degree in electrical engineering from South Dakota State University, Brookings, SD. He is currently a Senior Instrument Engineer with Science Systems and Applications, Inc., primarily working on the radiometric characterization and calibration of the reflective solar bands of the MODIS instruments on board the Terra and Aqua spacecraft. His research interests include sensor cross-calibration and validation.



Hongda Chen received the BS and MS degrees in electrical engineering from Beijing Institute of Technology, Beijing, China, in 1987 and 1990 respectively, and the PhD degree in information technology from George Mason University, Fairfax, VA, in 1999. He currently serves as a senior research scientist with Sigma Space Corporation, Lanham, MD, working on NASA EOS projects. His research interests include signal processing, data analysis, communications, fault diagnosis/prognosis and instrument calibrations.



Sriharsha Madhavan received the BE degree in electrical and electronics engineering from the University of Madras, Chennai, India in 2001 and the MS degree in electrical engineering from South Dakota State University, Brookings, SD in 2004. He is currently a senior member of the MODerate Resolution Imaging Spectroradiometer Characterization Support Team (MCST), Science Systems and Applications, Inc., Lanham, MD. He is also a PhD candidate in the Environmental and Geoinformation sciences program in George Mason University, Fairfax, VA.



Aisheng Wu received the BS degree in atmospheric science from the University of Science and Technology of China, Hefei, China, the MSc degree in atmospheric remote sensing from Chinese Academy of Science, Institute of Plateau Atmospheric Physics, Lanzhou, China, and PhD in soil science from the University of British Columbia, Vancouver, Canada. He is currently a senior scientist with MODIS Characterization Support Team/Sigma Space Corp., Lanham, MD.

James Kuyper: Biography and photograph not available.